

pubs.acs.org/ac Perspective

Advancing Evidence-Based Data Interpretation in UV-Vis and Fluorescence Analysis for Nanomaterials: An Analytical Chemistry Perspective

Max Wamsley, Shengli Zou, and Dongmao Zhang*

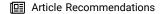


Cite This: Anal. Chem. 2023, 95, 17426–17437



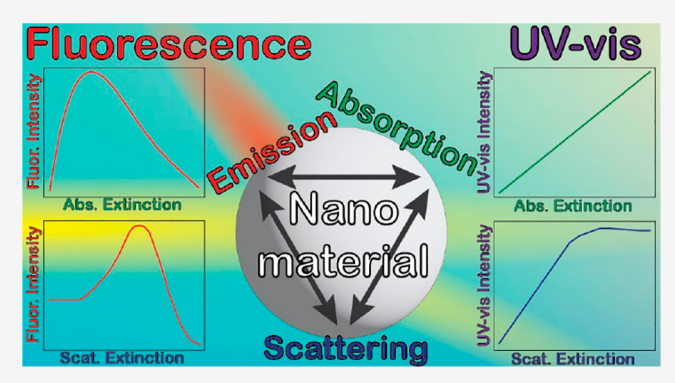
ACCESS I

III Metrics & More



s Supporting Information

ABSTRACT: UV—vis spectrophotometry and spectrofluorometry are indispensable tools in education, research, and industrial process controls with widespread applications in nanoscience encompassing diverse nanomaterials and fields. Nevertheless, the prevailing spectroscopic interpretations and analyses often exhibit ambiguity and errors, particularly evident in the nanoscience literature. This analytical chemistry Perspective focuses on fostering evidence-based data interpretation in experimental studies of materials' UV—vis absorption, scattering, and fluorescence properties. We begin by outlining common issues observed in UV—vis and fluorescence analysis. Subsequently, we provide a summary of recent advances in commercial UV—vis spectrophotometric and spectrofluorometric instruments, emphasizing their potential to



enhance scientific rigor in UV—vis and fluorescence analysis. Furthermore, we propose potential avenues for future developments in spectroscopic instrumentation and measurement strategies, aiming to further augment the utility of optical spectroscopy in nano research for samples where optical complexity surpasses existing tools. Through a targeted focus on the critical issues related to UV—vis and fluorescence properties of nanomaterials, this Perspective can serve as a valuable resource for researchers, educators, and practitioners.

INTRODUCTION

The interactions between photons and matter have long captivated scientists and researchers, standing as one of nature's most intriguing and profound phenomena. Optical spectroscopic techniques, dedicated to studying such interactions, have emerged as indispensable tools in scientific research, technology advancement, and education. Their applications in nano research are especially prominent because of the tunability in nanoparticle optical properties as a function of particle size, shapes, chemical composition, even internal packings and surface morphology including surface defect. 1-4 This unique photoelectronic property makes nanomaterials increasingly popular in diverse disciplines including energy, chemistry, medicine, environment, and materials sciences. Reliable quantification of nanomaterials' optical properties, including their absorption, scattering, and emission activities, is essential for rational nanomaterials design and applications.

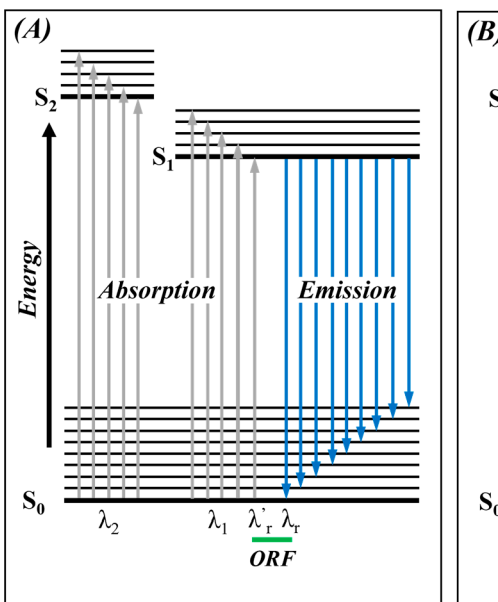
Despite the extensive history and broad utility of UV—vis and fluorescence techniques, numerous issues are associated with the analysis of spectral data obtained from solutions containing nanoscale or larger materials. A significant distinction of small dissolved molecular chromophores and fluorophores from their respective nanoparticle counterparts is the escalating scattering activities observed in the solutions

containing nanoscale or larger analytes. In a simple assumption, the scattering cross section of a nonabsorbing particle is proportional to the square of its volume. While small dissolved molecular chromophores, due to their small sizes, can be treated as pure absorbers in UV-vis measurements, scattering by nanoparticles, owing to their large sizes, can be very strong, and the cross section can be comparable to or even surpass their absorption cross-section and dominant in extinction. The high scattering activity complicates the UVvis and fluorescence spectral acquisition and interpretation. As one example, the long-held general practice in assigning UVvis spectra obtained with dissolved molecular chromophore as an absorbance spectrum is generally invalid for solutions containing nanoscale or larger materials. This is because both absorption and scattering contribute to the UV-vis extinction spectra.⁸⁻¹² Further complication arises if one considers interference of forward scattered and emitted photons in the

Received: August 4, 2023 Revised: October 30, 2023 Accepted: October 31, 2023 Published: November 16, 2023







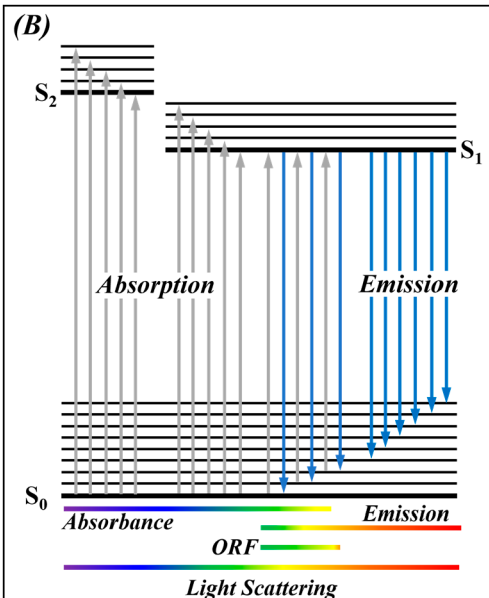


Figure 1. (A) Conventional and (B) augmented Jablonski energy diagram. Intersystem crossing and phosphorescence are omitted for clarity. Light absorption and emission are depicted by gray lines with upward arrows and blue lines with downward arrows, respectively. The absorption by hot molecules shown on the ORF wavelength region is indicated by the horizontal lines with gradient color.

UV—vis spectral acquisition. $^{10-12}$ However, it has been prevalent in current literature to assign the UV—vis spectrum as absorbance or absorption extinction spectrum, $^{13-19}$ even for samples likely having strong scattering activities. The impact on the scattering activity of numerous nanomaterials has been published extensively in previous works. $^{10-12,20-22}$

Reliable quantification of nanoparticles absorption, scattering, and emission activities is essential for rational materials characterization, design, and applications as these optical processes differ significantly in their causes, effects, and applications. As examples, metal oxide nanoparticles with strong scattering activities in the UV ranges has been used extensively as sun block, while plasmonic nanoparticles find utilities in biosensing due to their strong scattering in the visible to infrared wavelength range. 23-25 The applications of photoactive nanoparticles, referring to chromogenic and fluorogenic nanomaterials, are even more diverse, ranging from photocatalysis, ^{26–28} photoluminescence, ^{29–31} photodynamic therapy, ^{32–34} photoelectronics, ^{35–38} and photothermal energy harvesting, ^{39–41} just to name a few. For these applications, it is the absorbed photons, not the scattered photons, that are directly responsible for chemical reactions in photocatalysis, light emission in photoluminescence, and singlet oxygen generation in photodynamic therapy. However, light scattering can alter the propagation direction and path length of photons within samples, affecting the location and probability (thereby, the amount) of photon absorption and emission (for fluorogenic nanoparticles). 11,42-45 As a result, this scattering indirectly impacts the performance of photoactivated applications in these samples.

The complexity of scattering in the quantification of materials' absorption and emission properties has been widely acknowledged for a long time. ^{10–12,46} Several experimental approaches have been proposed to enhance the analysis of analyte optical properties in turbid solutions, including absorption, scattering, and fluorescence activities as well as scattering and fluorescence depolarizations or anisotropy. The

latter two terms are interchangeable as measures of the spatial distribution of scattered and emitted light.⁴⁷ For example, Lin et al. reported a two-channel spectrometer to quantify the UV—vis absorption and scattering extinction contribution to the plasmonic nanoparticle UV—vis extinction spectrum.⁴⁸ Home-developed integrating-sphere-based UV—vis spectrometers have also been used for measuring sample UV—vis absorbance.^{45,49–53} However, most of these earlier techniques rely on custom-built instruments or accessories, making it challenging for educators and researchers to adopt, verify, and implement them. Consequently, ambiguous and erroneous data interpretations persist despite these technical advances.^{54,55}

The objective of this analytical chemistry Perspective is to shed light on the challenges and opportunities of UV-vis spectrophotometric and spectrofluorometric analysis, especially for samples containing nanoscale or larger materials. To facilitate the independent verification and broad adoption, we limit our discussion to techniques utilizing broadly accessible commercial UV-vis and fluorescence instruments along with commonly available commercial accessories for these instruments. Our intention is to empower researchers to enhance the scientific rigor of spectral acquisition and analysis using readily accessible tools, thereby advancing evidence-based data interpretation. This Perspective is organized into four sections. First, a primer will be provided to explain the optical processes in the context of spectroscopic measurements with solution samples. This background knowledge is crucial for developing a mechanistic understanding of the signal origins in conventional UV-vis and fluorescence measurements and the challenges in spectral analysis. Second, a concise literature review will be presented, highlighting common literature examples of ambiguous and even erroneous spectral interpretation and analysis. By examining these cases, we can gain insights into potential pitfalls and challenges faced in the characterization of nanomaterial optical properties. Third, a critical assessment is provided on the strengths and weaknesses

of the recent spectroscopic techniques developed using commercial UV—vis spectrophotometric and spectrofluorometric methods. By evaluating these advancements, we can identify areas where improvements can be made and where current techniques excel. Finally, an outlook is provided on the future use of optical spectroscopy in education and research and highlights potentially impactful research topics. This section aims to inspire and guide future investigations in utilizing optical spectroscopy for nanoscale applications, identifying promising avenues for further exploration.

PHOTO AND MATTER INTERACTIONS, A PRIMER FOR OPTICAL SPECTROSCOPIC TECHNIQUES

Augmented Jablonski Energy Diagram. The conventional Jablonski energy diagram (Figure 1A), extensively used in student textbooks and literature, is limited in depicting the complexity of light interactions with nanoscale and larger materials concerning light absorption, scattering, and emission. All materials can be classified into four groups based on their optical complexities under illumination with UV—vis light: (1) absorbers with negligible light scattering and emission activities, (2) scatterers with no significant absorption or emission, (3) materials that both absorb and scatter light, and (4) materials that absorb, scatter, and emit light.

To facilitate a comprehensive discussion on photophysical processes resulting from light irradiation on nanomaterials, we assume that the nanoparticles exhibit fluorescence activity and possess overlapping excitation, scattering, and emission spectra. For these samples, the optical processes under UVvis excitation can be depicted with an augmented Jablonski's energy diagram (Figure 1B) that includes the light absorption, scattering, and fluorescence emission. Beside the scattering that occurs across all excitation wavelengths, another new feature in the augmented Jablonski diagram is light absorption and emission by hot molecules, which are the molecules in the ground electronic state but at excited vibrational and rotational states. Based on Boltzmann's distribution, fluorophores at ground electronic states can also be at excited vibrational/or rotational states. The light absorption by hot molecules can push the red-edge absorption wavelength to wavelengths longer than the blue-edge emission wavelength, which is why fluorophore fluorescence excitation and emission spectra commonly have an overlapping wavelength region. Exciting fluorophores with light in the overlapping wavelength regions simultaneously produces anti-Stokes-shifted fluorescence (ASSF), on-resonance fluorescence (ORF), and Stokes-shifted fluorescence (SSF). 20,21,56,57 The terms ASSF, ORF, and SSF refer to fluorescence emission wavelengths that are shorter than, equal to, and longer than the excitation wavelength, respectively. Experimental detection of ASSF, ORF, and SSF is straightforward using a spectrofluorometer by scanning the detection wavelength continuously from the anti-Stokes-shifted (blue) side to the Stokes's shifted (red) side of the excitation wavelength that is at the wavelength region the fluorophore both absorb and emit. 21,57,58

The red-edge absorption wavelength and the blue-edge emission wavelength depicted in the conventional Jablonski energy diagram (Figure 1A) are identical, and it corresponds to the energy difference between the ground and first excited electronic states, with both states assumed to be in their lowest vibrational states. Therefore, this energy diagram predicts the appearance of ORF. Evidently, however, this conventional Jablonski energy diagram not only fails to explain the presence

of concurrent ASSF, ORF, and SSF emission that have been observed for numerous molecular and nanoparticle fluorophores, $^{21,57,59-61}$ it also oversimplifies the ORF. Instead of a delta function at a single ORF wavelength $\lambda_{\rm r}$ predicted in the conventional Jablonski energy diagram (Figure 1A), the full width at half-maximum of experimental ORF spectra varies from a few nanometers to tens of nanometers. $^{21,57-59}$

For discussion convenience, we divide the UV-vis wavelength depicted in the augmented Jablonski energy diagram into three wavelength regions (Figure 1B) based on the sample optical complexity under resonance excitation and detection conditions: a blue region where the analyte absorbs and scatters but does not emit, an ORF region where the analyte absorbs, scatters, and emits, and a red wavelength region where the analytes scatter light and emit but do not absorb. Note that the sample optical complexity in these wavelength regions varies depending on the spectroscopic techniques. For instance, for UV-vis measurements that have no detection monochromator, fluorescent nanoparticles depicted in the augmented Jablonski energy diagram function as simultaneous light absorbers, scatterers, and emitters in the blue and ORF wavelength regions, while they solely act as pure scatterers in the red wavelength region. This detailed conceptual understanding of nanoparticle optical properties under different conditions is essential not only for qualitative optical spectral interpretation but also for the quantification of materials' optical properties.

■ CURRENT UV—Vis SPECTROPHOTOMETRIC AND SPECTROFLUOROMETRIC ANALYSIS IN NANO RESEARCH

UV–Vis Spectroscopy. The century-old Beer's law (eq 1) is the mathematical model used for analyzing UV–vis spectra, which states that the UV–vis extinction $(E_{\rm T}(\lambda_{\rm x}))$ is proportional to the materials' molar extinction coefficient $\varepsilon(\lambda_{\rm x})$, concentration C, and cuvette path length (l). The subscript T in $E_{\rm T}(\lambda_{\rm x})$ is to highlight the fact that this equation is a physical chemistry model that can deviate significantly from the analytical signal, even when the experimental extinction is within the linear dynamic range (LDR) specified by the instrument vendors.

$$E_{\mathrm{T}}(\lambda_{\mathrm{x}}) = l_{\mathrm{F}}(\lambda_{\mathrm{x}})C \tag{1}$$

The analytical chemistry model (eq 2) is far more complex than Beer's law. eq 2 is derived by parametrizing the experimental UV–vis extinction $E_{\rm UV}(\lambda_{\rm x})$ as the analyte extinction, scattering extinction, and sampling conditions. For generality, the analytes are assumed to be simultaneous absorbers, scatterers, and emitters under excitation wavelength $\lambda_{\rm x}$.

$$\begin{split} E_{\text{UV}}(\lambda_{\text{x}}) &= -\text{log}[I_0(\lambda_{\text{x}})10^{-(S_a(\lambda_{\text{x}}) + A_a(\lambda_{\text{x}}))} + \eta S(\lambda_{\text{x}})I_S(\lambda_{\text{x}}) \\ &+ \int \eta_{\text{F}}(\lambda_{\text{x}}, \lambda_{\text{m}})I_F(\lambda_{\text{x}}, \lambda_{\text{m}})d_{\text{m}}]I_0(\lambda_{\text{x}}) \end{split} \tag{2}$$

The solvent UV—vis absorption and scattering extinction are assumed to be negligible in comparison to the respective counterparts $A_{\rm a}(\lambda_{\rm x})$ and $S_{\rm a}(\lambda_{\rm x})$ by the nanoparticle analytes. This is generally the case in practical UV—vis measurements. $I_{\rm S}(\lambda_{\rm x})$ is the scattered light intensity of the sample solutions. $\eta_{\rm S}(\lambda_{\rm x})$ represents the fraction of the scattered light reaching the detector used in the UV—vis spectrophotometer. $I_{\rm F}(\lambda_{\rm x}\lambda_{\rm m})$ is the total fluorescence at the emission wavelength $(\lambda_{\rm m})$ and

excited with the excitation wavelength (λ_x) , while $\eta_F(\lambda_x \lambda_m)$ represents the fraction of the fluorescence reaching the UV-vis detector. The integration is necessary due to the absence of detector monochromator, any fluorescence photons reaching the detector, regardless of their wavelength, interfere with experimental UV-vis acquisition.

Experimental confirmation of the scattering and fluorescence interference on UV-vis measurements is straightforward by studying the sample UV-vis LDR and by comparing the conventional UV-vis spectrum with that acquired with the integrating-sphere-assisted UV-vis method (ISUV). 10-12 For molecular chromophores that are approximately pure absorbers, the experimental UV-vis spectrum maintains excellent linearity if the sample optical density is within the instrument LDR specified by the vendor (Figure S1(A-D)). However, for nanoparticles that are scatterers, simultaneous absorbers and scatterers, or simultaneous absorbers, scatterers, and emitters, the upper limit of the experimental LDR can be significantly lower than that for the pure absorbers (Figure S1(E-L)). 12 Their experimental LDR upper limit depends not only on particle sizes but also on the excitation wavelengths, complicating the UV-vis spectrum data interpretation and analysis.

There are countless ambiguous and even erroneous UV-vis spectral interpretations and analyses in nano research. It has been common practice to interpretate, explicitly or implicitly, the UV-vis spectra obtained with solutions containing nanoscale and larger materials as absorbance spectra for quantification of nanomaterials' absorption activities, 62-64 nanocrystal band gaps, ⁶⁵⁻⁶⁷ as well as for identification of broadband absorbers. ⁶⁸⁻⁷⁰ The latter is based on the observation that the sample UV-vis spectrum exhibits a similar intensity across a broad range of wavelengths. This approach is problematic, because UV-vis measurements do not directly provide a direct measurement of absorbance or absorption extinction. Instead, it is the sum of the absorption and scattering extinctions in the best situation. Indeed, the wavelength-insensitive UV-vis responses may be attributed to the intrinsic scattering extinction or spectral distortion caused by forward scattered and fluorescence light. As an example, the UV-vis features of the fluorescent polystyrene nanoparticles become much more wavelength-independent at high concentrations compared to those at low concentrations (Figure S1I).12

Another recurring concern in nanoscience literature is the calculation of materials' extinction coefficients using experimental UV—vis spectra without adequately accounting for potential spectral distortions caused by scattering and fluorescence interferences. It is essential to recognize that experimental UV—vis spectra do not necessarily follow Beer's law even when the apparent intensity is within the instrument LDR. Fortunately, recent advancements made using broadly available commercial UV—vis and fluorescence instruments have paved the way for elevating the rigor of UV—vis spectral analysis (vide infra).

Fluorescence Spectroscopy. Spectrofluorometers are likely the most versatile instruments. A commercial spectrofluorometer equipped with common accessories such as an integrating sphere and excitation and detection linear polarizer allows for a variety of materials characterization applications. The discussion in this subsection is limited to the fluorescence emission intensity spectrum, as it is the most applied spectrofluorometric analysis.

To facilitate discussion, it would be beneficial to revisit the mathematical models frequently employed in fluorescence spectral analysis. eq 3 is the popular textbook model based on the definition of the fluorescence quantum yield $Q(\lambda_x, \lambda_m)$, ratio of the number of emitted photons $I(\lambda_m)/k_m(\lambda_m)$ versus the number of absorbed photons $I(\lambda_x)(1-10^{-A(\lambda_x)})/k_x(\lambda_x)$. $K(\lambda_x,\lambda_m)$ is a constant that contains the combined contribution from (1) the conversion factors $k_m(\lambda_x)$ and $k_x(\lambda_x)$, the two variables converting the emitted light intensity $I(\lambda_m)$ and absorbed light intensity $I(\lambda_m)(1-10^{-A(\lambda_n)})$ into the number of emitted and absorbed photons and (2) the instrument excitation and detection efficiency, including the detector quantum efficiency at each wavelength. To be general, we assume that the fluorescence quantum yield $Q(\lambda_x,\lambda_m)$ is a function of both the excitation wavelength λ_x and emission wavelength $\lambda_{\rm m}$. eq 3 can be simplified into eq 4 when the $A(\lambda_{\rm x})$ < 0.05 and by replacing $A(\lambda_{\rm x})$ with fluorophore concentration using eq 1.71 For simplicity, $K'(\lambda_{\rm x},\lambda_{\rm m})$ is used, which equals $2.303 K(\lambda_{\rm x}, \lambda_{\rm m}).$

$$I(\lambda_{\rm v}, \lambda_{\rm m}) = K(\lambda_{\rm v}, \lambda_{\rm m}) Q(\lambda_{\rm v}, \lambda_{\rm m}) I(\lambda_{\rm v}) (1 - 10^{-A(\lambda_{\rm x})}) \tag{3}$$

$$I(\lambda_{x}, \lambda_{m}) = K'(\lambda_{x}, \lambda_{m})I(\lambda_{x})Q(\lambda_{x}, \lambda_{m})C_{f}$$
(4)

$$\frac{I_0(\lambda_x, \lambda_m)}{I_q(\lambda_x, \lambda_m)} = (1 + k_q \tau_0[q])(1 + K_a[q])$$
(5)

eq 4 has been used extensively in analytical and physical chemistry. Indeed, the popular generalized Stern-Volmer's (SV) equation (eq 5) is rooted in eq 4. The $(1 + K_a[q])$ term depicts the impact of static quenching (i.e., the fraction of fluorophores that bind to the ligand and become nonfluorescent). In other words, this term describes the effect of ligand-fluorophore interactions on the concentration of the fluorophore C_f in eq 4. The addition of a static quencher reduces the concentration of the free fluorophore to $C_f/(1 +$ $K_a[q]$), where K_a is the equilibrium fluorophore and the ligand binding constant. The term $1 + k_q \tau_0[q]$ in eq 5 depicts the impact of dynamic quenching (i.e., the collisions between the excited fluorophores and ligands that lead to nonradiative relaxation). This term describes the effect of the ligand/ fluorophore interaction on $Q(\lambda_x \lambda_m)$ in eq 4. The presence of a dynamic quencher reduces the fluorescence quantum yield from $Q(\lambda_x \lambda_m)$ to $Q(\lambda_x \lambda_m)/(1 + k_q \tau_0[q])$.

Since eq 3 serves as the fundamental basis for eq 4 and eq 5, examining the validity of eq 3 in practical fluorescence measurements reveals the challenges both in general fluorescence analysis and specifically within the context of nano research. Indeed, this model fails even for the simplest fluorescent solutions that contain only one molecular fluorophore. eq 3 predicts that the sample fluorescence monotonically increases with increasing fluorophore absorption. However, in practice, the experimental fluorescence intensity can decrease with increasing fluorophore light absorption, even when the solution absorbance surpassing the threshold value is as low as 0.3 (Figure S2).⁷²

Further complications arise if the samples contain chromogenic species that absorb but do not emit. The chromophore reduces fluorescence intensity by absorbing the excitation and/or emission photons but does not contribute to fluorescence signal generation. The impacts of fluorophore and chromophore absorption on the fluorescence emission follows a first-principles model (eq 6a or eq 6b) developed based on

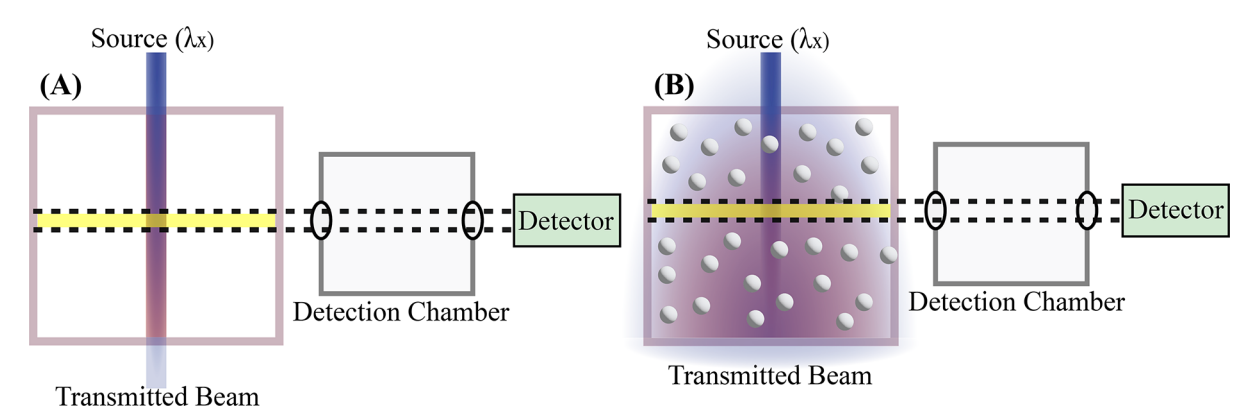


Figure 2. Simplified excitation and detection scheme of typical commercial spectrofluorometers for (A) fluorescent samples that contain no significant light scatterers (simultaneous absorber and emitter) and (B) fluorescent samples that do contain significant light scatterers (simultaneous scatterer, absorber, and emitter). The two pinholes on the detection chamber represent the collective effects of the optical elements that impose spatial constraints on the detected fluorescence photons. Only a fraction of photons generated in the effective sampling path length (l_s) can reach the detector and produce fluorescence signal. The effective volume available for detection is represented by the yellow box. 12

the pinhole effect (Figure 2A) in practical spectrofluorometric acquisition. This model considers the absorption inner filter effect arising from the sample absorption (by both the fluorophore and chromophore) of the excitation ($A_{x,s}$) and emission ($A_{m,s}$) photons along the effective fluorescence excitation (d_x) and emission (d_m) path lengths. The excitation wavelength absorption by the fluorophore at the excitation wavelength. Subscripts x and x in the absorbance terms refer to the excitation and emission wavelengths, respectively. The subscripts x and x in the absorbance terms refer to the absorbance by the fluorophore or the sample and are interchangeable if the sample solution contains one molecular fluorophore.

$$I(\lambda_{x}, \lambda_{m}) = I(\lambda_{x})Q(\lambda_{x}, \lambda_{m})K(\lambda_{x}, \lambda_{m})A_{x,f}10^{-(A_{x,s}d_{x} + A_{m,s}d_{m})}$$
(6a)

$$I(\lambda_{\rm x},\,\lambda_{\rm m})=I(\lambda_{\rm x})K'(\lambda_{\rm x},\,\lambda_{\rm m})C_{\rm f}10^{-(A_{\rm x,s}d_{\rm x}+A_{\rm m,s}d_{\rm m})} \eqno(6b)$$

eq 6b is obtained by simply grouping the terms that are constants in applications where the sample fluorescence quantum yield is constant and the sample absorbance follows Beer's law.^{72,73} Experimental validation of eq 6a has been conducted using a fluorophore both with and without addition of a chromogenic species that has no direct chromophore and fluorophore interactions.^{72,74}

eq 6a or eq 6b can be viewed as an analytical chemistry model for analyzing fluorescence spectra obtained with samples with no significant scattering activities. It is far more effective than the physical chemistry model (eq 3) to explain the correlation between sample light absorption and fluorescence emission. While the physical chemistry model is effective to explain the origin of fluorescence emission (i.e., light absorption triggers fluorescence emission) it fails to capture the fact that absorption can also attenuate the fluorescence photons.^{72,75}

The fact that chromophores can reduce fluorescence intensity without direct fluorophore/chromophore interactions (i.e., through either fluorophore binding or collision with the fluorophores) cautions the use of Stern-Volmer's (SV) equation for fluorescence study of intermolecular interactions. Indeed, the SV equation is effective only under a series of stringent conditions, some of which have been discussed in an excellent review by Gehlen.⁷⁶ Unfortunately, such conditions

are very difficult, or even impossible, to meet or verify for solutions used in nano research. Regardless of the possibility of static and dynamic quenching, as modeled by the SV equation, the addition of light-absorbing nanoparticles to fluorescent solutions or the incorporation of absorbing molecules into fluorescent nanoparticles will attenuate the sample fluorescence. This occurs due to the absorption inner filter effect that becomes significant when the sample absorption is higher than a threshold value as small as 0.05. A,72,78

$$I(\lambda_{x}, \lambda_{m}) = I(\lambda_{x})Q(\lambda_{x}, \lambda_{m})K(\lambda_{x}, \lambda_{m})k_{s}(S)A_{x,f}$$

$$10^{-(A_{x,s}d_{x} + A_{m,s}d_{m}) - \eta(S)}$$
(7)

Light scattering can also perturb the fluorescence intensity by modifying the fluorescence signal generation and detection. Although scattering itself does not produce fluorescence, as rightfully implied by eq 3, it can change the locations and number of photons absorbed as well as the path of emitted photons (Figure 2B). Compared to the light absorption, however, the impact of scattering on fluorescence is significantly smaller. Empirically, the effects of light scattering on the fluorophore fluorescence can be modeled by adding two additional terms into eq 6a, depicting two competing effects of scattering on fluorophore fluorescence. The $\eta(S)$ term in eq 7 represents the scattering inner filter effect, depicting the extent of fluorescence signal reduction caused by the scattering on the excitation photons propagating to the effective sampling path length defined by the instrument pinhole effects (Figure 2B). Note that $\eta(S)$ is invariably larger than zero but should be significantly smaller than the scattering extinction in practical fluorescence acquisition. Unlike light absorption, which terminates the excitation or emission photons, scattering changes only the propagation paths of the excitation photons. These scattered photons remain effective for fluorescence generation before exiting the cuvette, and some of these emitted photons can propagate to the fluorescence detector, partially compensating for the scattering inner filter effect on fluorescence signal reduction.

On the other hand, the $k_s(S)$ term in eq 7 is the effective sampling path length enhancement factor, which is invariably larger than 1, due to longer path lengths of the scattered photons traveling within the effective sampling path length defined by the instrument pinhole effects. Therefore, the

overall effect of scattering on fluorescence intensity depends on these two competing factors, which can enhance, reduce, or have no significant impact on the experimental fluorescence as experimentally demonstrated with Eosin Y mixed with nanoparticle (Figure S3).¹²

It is a common observation that addition of nanomaterials to fluorophore-containing solutions modifies (enhances or reduces) sample fluorescence. The However, the influence of absorption and scattering on the fluorescence signal has often been overlooked or insufficiently addressed. The failure to correct the absorption inner filter effect (IFE) typically results in an underestimation of the sample's true fluorescence intensity or an overestimation of nanoparticle-induced fluorescence quenching. Since the impact of scattering on sample fluorescence intensity is usually small, correcting only the sample IFE caused by sample absorption is usually adequate for most applications. To achieve this correction for nanomaterial samples one must be able to quantify the material's absorption and scattering extinctions in the UV-vis spectrum of the sample as outlined, in Figure 3.

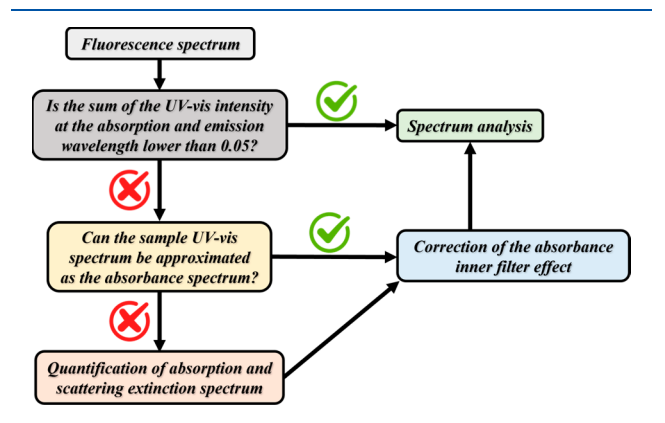


Figure 3. Workflow for correction of the sample absorption inner filter effect on fluorescence spectra for samples where the sample scattering extinction is small (<0.5) and scatterers' size are small $(\le300 \text{ nm})$.

Another area that also suffers from ambiguity is the effect of stimuli treatments on the fluorescence properties of the photoluminescent nanoparticles. Example stimuli treatments include temperature, solvent, and electrolytes, including addition of acid and base for changing sample pH.85-89 It is not uncommon for researchers to attribute the fluorescence intensity changes as the changes in the fluorophore quantum yield. However, as shown in the expanded analytical chemistry model (eq 7), the fluorescence spectrum (both spectral intensity and shape) depends on multiple parameters, including the fluorescence quantum yield, fluorophore and sample absorbance, and sample scattering. All latter two parameters can also be susceptible to stimuli treatments, offering an alternative explanation to the fluorescence spectral changes. As an example, our recent study revealed that while the apparent fluorescence intensity generally decreases with increasing temperatures, the fluorescence quantum yield can increase or decrease depending on the excitation and emission wavelengths.⁷³ Indeed, a decrease in fluorescence intensity does not necessarily indicate a decrease in the quantum yield, nor does an increase in fluorescence intensity imply an increase in the quantum yield. The quantum yield can increase even when the intensity decreases if the decrease of emitted photons is slower than the decrease of the absorbed photons. Conversely, the quantum yield can decrease even when the fluorescence intensity increases if the increase in emitted photons is slower than the increase in absorbed excitation photons. To improve the reliability of fluorescence analysis of stimuli treatment on the nanoparticle emissivity, one should have a full characterization of the nanoparticle absorption and scattering properties, as the two optical processes affect the emission photon generation and detection.

■ RECENT PROGRESS IN UV—Vis SPECTROPHOTOMETER- AND SPECTROFLUOROMETER-BASED MEASUREMENTS

ISUV and Integrating-Sphere-Assisted Resonance Synchronous Spectroscopy (ISARS). The recently devel-

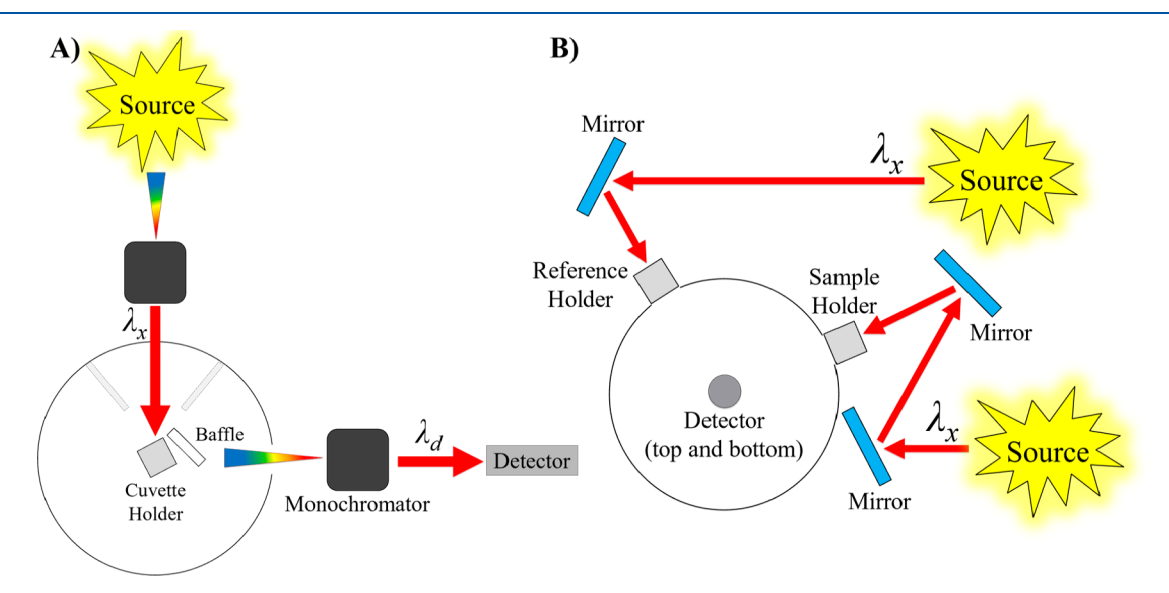


Figure 4. (A) Scheme of ISARS spectral acquisition. The excitation and detection wavelengths are kept the same (resonance) and varied simultaneously (synchronous) during the ISARS data acquisition. (B) Sampling scheme of the commercial IS-equipped UV-vis spectrophotometer.⁴⁵

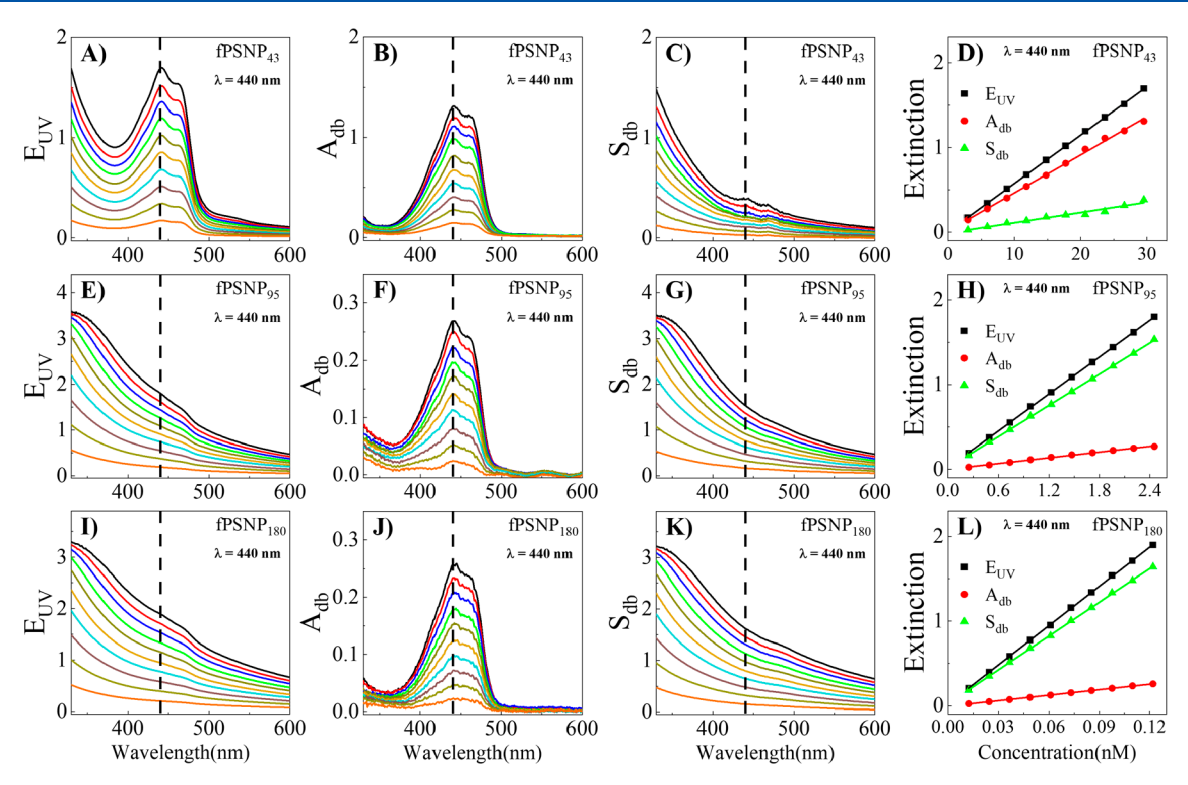


Figure 5. $(E_{\rm UV})$ experimental extinction spectra of (A) fPSNP₄₃, (E) fPSNP₉₅, and (I) fPSNP₁₈₀. (B, F, J) UV-vis absorption extinction spectra derived from $(A_{\rm db})$ ISARS-based absorbance spectra for the samples shown in (A), (E), (I), respectively. $(S_{\rm db})$ UV-vis scattering extinction spectra of (C) fPSNP₄₃, (G) fPSNP₉₅, and (K) fPSNP₁₈₀ samples, which were obtained by subtracting the experimental extinction spectrum in (A, E, I) by the corresponding absorption extinction spectrum in (B, F, J), respectively. (D, H, L) UV-vis total extinction, absorption extinction, and scattering extinction intensity at 440 nm for the fPSNP₄₃, fPSNP₉₅, and fPSNP₁₈₀, respectively. (PSNP₁₈₀)

oped ISUV and ISARS methods (Figure 4), utilizing commercial UV—vis spectrophotometers and spectrofluorometers, respectively, offer convenient approaches for enhancing UV—vis spectral interpretation and analysis. The integrating spheres needed for ISARS and ISUV spectroscopic measurements are both commercially available from their respective vendors. Integrating spheres have been used in UV—vis-based spectroscopic acquisition for experimental quantification of the diffused UV—vis reflectance/absorption of the solid samples. Phenomenant of the integrating-sphere-based diffuse reflectance/absorption quantification is that the former detects forward propagated light. In contrast, the quantification of reflectance/absorption measures the light propagated backward to the integrating spheres when light is illuminated on solid samples.

Integrating spheres are common accessories for the fluorescence QY analysis. The key differences between the QY and ISARS measurements are the excitation and detection wavelength controls. The excitation wavelength is fixed in the QY quantification, but the detection wavelength usually varies from 5 to 10 nm anti-Stokes's shifted from the excitation wavelength to the expected red edge of the fluorescence spectrum. In contrast, both the excitation and emission wavelengths vary in the ISARS measurements and are kept identical during the excitation spectroscopic acquisition. As a result, the ISARS collects all scattered and transmitted lights, together with ORF photons, if the excitation wavelength is in the sample ORF-active wavelength region. Since the ORF quantum yield is small (<0.1), 57,59,60 its impact on the ISARS-based absorbance quantification is negligible in practical applications. In other words, ISARS selectively detects

materials' light absorption. Detailed procedures for conversion of the ISARS-based sample absorbance to its double-beam UV—vis absorbance and subsequent separation of the sample double beam UV—vis extinction spectra into its absorption and scattering extinction spectra have been recently reported (Figure 5).⁴⁵

Taken together, the ISUV spectra and ISARS methodology pave ways for evidence-based UV—vis spectral interpretation and analysis (Figure 6). The agreement between the sample UV—vis and ISUV spectra justify the assignment of UV—vis spectra as the absorbance spectrum, while the agreement of sample and solvent ISARS offers justification for assigning an experimental spectrum as the scattering extinction spectrum.

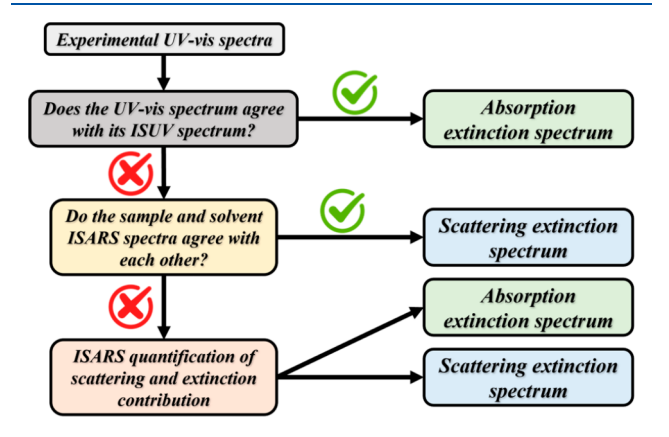


Figure 6. Workflow for enhancing evidence-based UV-vis spectral interpretation.

For samples that do not belong in either category, a combined UV—vis and ISARS study is needed for reliable data interpretation.

Linearly Polarized Resonance Synchronous (LPRS) and Linearly Polarized anti-Stokes-Shifted, on-Resonance, and Stokes-Shifted (LPAOS) Spectroscopy. LPRS and LPAOS spectroscopy are two recently developed spectrofluorometer-based technologies that were previously referred to as polarized resonance synchronous spectroscopy (PRS2) and polarized anti-Stokes shifted, on-resonance, and Stokes-shifted (PAOS), respectively. 21,56 These advancements have been achieved by leveraging the independent controls of wavelength and polarization in excitation and detection light within commercial spectrofluorometers. Like resonance synchronous and ISARS spectroscopic techniques, the LPRS spectrum is obtained by maintaining identical excitation and detection wavelengths during spectral acquisition. However, the resonance synchronous and ISARS utilizes nonpolarized light for excitation and detection, while the LPRS acquisition employs linearly polarized light for both excitation and detection (Figure S4(II)). The LPRS signal encodes the sample absorption, scattering, and emission intensity occurring at the excitation wavelength. \$6,61,93,94 While the scattering and ORF increases LPRS intensity, light absorption reduces the LPRS signal through the absorption inner filter effect. LPAOS also employs linearly polarized light for both excitation and detection. Unlike the LPRS acquisition where the excitation and detection wavelengths are kept identical, the detection wavelength in current LPAOS measurement varies continuously anti-Stokes side to the Stokes-shifted side of the excitation wavelength.²¹

The emerging LPRS and LPAOS methodologies have greatly expanded the utility of spectrofluorometers for extracting information that was previously inaccessible. The key new information enabled by these two techniques includes: (1) ORF intensity, quantum yield, and depolarization spectra; ^{60,95} (2) scattering intensity and depolarization spectra; ^{20,21,56,60,61,93} and (3) absorption and scattering extinction contribution to their extinction spectrum (Figure S5). ^{21,59,74} Note that the LPRS and LPAOS quantification of absorption and scattering extinction is valid only when the sample light scattering can be approximated as Rayleigh scattering. In such a case, the spatial distribution of the scattered light can be evaluated based on the scattering depolarization spectrum.

OUTLOOKS FOR IMPROVING THE RELIABLITY AND UTILITIES OF UV—Vis SPECTROPHOTOMETRIC AND SPECTROFLUOROMETRIC TECHNIQUES

UV-Vis Nomenclature and Data Presentation. The casual and inconsistent nomenclature and data presentation undoubtedly contribute to the widespread ambiguous interpretation and analysis of the UV-vis spectra. Spectra are often named based on the method of data acquisition or their underlying mechanistic origins. The data obtained with UV-vis spectrophotometers are referred to by various names in the current literature, such as "UV-vis spectrum," "UV-vis extinction spectrum," and most commonly "UV-vis absorbance spectrum." Clearly, the as-acquired spectrum should be referred to as a "UV-vis spectrum" to indicate that the data was obtained using a UV-vis spectrophotometer while

acknowledging that the reliability and the underlying physical origins of the spectral features are yet to be investigated. The term "UV-vis extinction spectrum" should be reserved for the UV-vis spectra that are known, through either prior knowledge or experimental confirmation, to be free of significant forward scattering and fluorescence interference and are thereby the sum of absorption extinction and scattering extinction. The term "UV-vis absorbance" or "absorption extinction spectrum" is even more specific than the UV-vis extinction spectrum and is designated to spectra obtained with samples that have been proven to exhibit no significant scattering extinctions. Due to the overuse and misuse of the term "UV-vis absorbance spectrum", we advocate to eliminate this term in UV-vis education and research and to instead use "absorption extinction spectrum" for the UV-vis spectra proven to be free of significant scattering extinction contribution. With the advent of ISUV and ISARS spectroscopic techniques, it is now entirely possible to conduct evidence-based UV-vis spectral interpretation with the workflow outlined in Figure 6.

Another important step in mitigating ambiguous UV—vis data analysis is to report the as-acquired UV—vis spectra with clearly labeled spectral intensities, rather than solely relying on normalized UV—vis data or simply ignore the scale of the UV—vis intensity. In nano science literature, it has been quite common to present normalized or arbitrarily scaled and/or baseline-offset spectra obtained from materials of varying sizes, concentrations, and compositions in the same figure. While these approaches might be effective to highlight spectral differences among the samples, it can obscure potential issues in data reliability as UV—vis spectra can be highly distorted even when the sample UV—vis intensity is within the instrument LDR. 10–12 To promote evidence-based spectral interpretation, we believe it is imperative to avoid reporting the processed UV—vis spectra without the as-acquired spectra either in the Supporting Information or in the main text.

Nomenclature of Resonance Synchronous Spectrum. Since its initial mention in the seminar work on resonance synchronous detection of porphyrin aggregation by Collings et al., 99 the term "resonance light scattering" (RLS) has gained popularity in the literature as a reference to "resonance synchronous spectrum and technique". 100–102 The term "resonance light scattering" implies that the resonance synchronous spectrum signal arises from sample light scattering, emphasizing the mechanistic origins of the observed phenomenon. In contrast, the term "resonance synchronous spectrum" is based on the method of spectral acquisition with no reference to the spectral signal origins.

We advocate the term "resonance synchronous spectrum" and urge the research community to avoid the use of RLS to refer to the data obtained with the spectrofluorometer in the resonance synchronous mode. The signal origin of resonance synchronous spectrum is highly complicated, as it involves the complex interplay among sample light absorption, scattering, and on-resonance emission. S6,74,95 As examples, the resonance synchronous spectra of molecular chromophores can be significantly lower than that of the solvent controls in the wavelength region that the chromophore absorbs. S8,99,103 Assigning the resonance synchronous spectrum as RLS spectrum would lead to the wrong conclusion that a molecular chromophore has a negative scattering! Another example is that the resonance synchronous spectrum of molecular fluorophores can be totally dominated by fluorophore

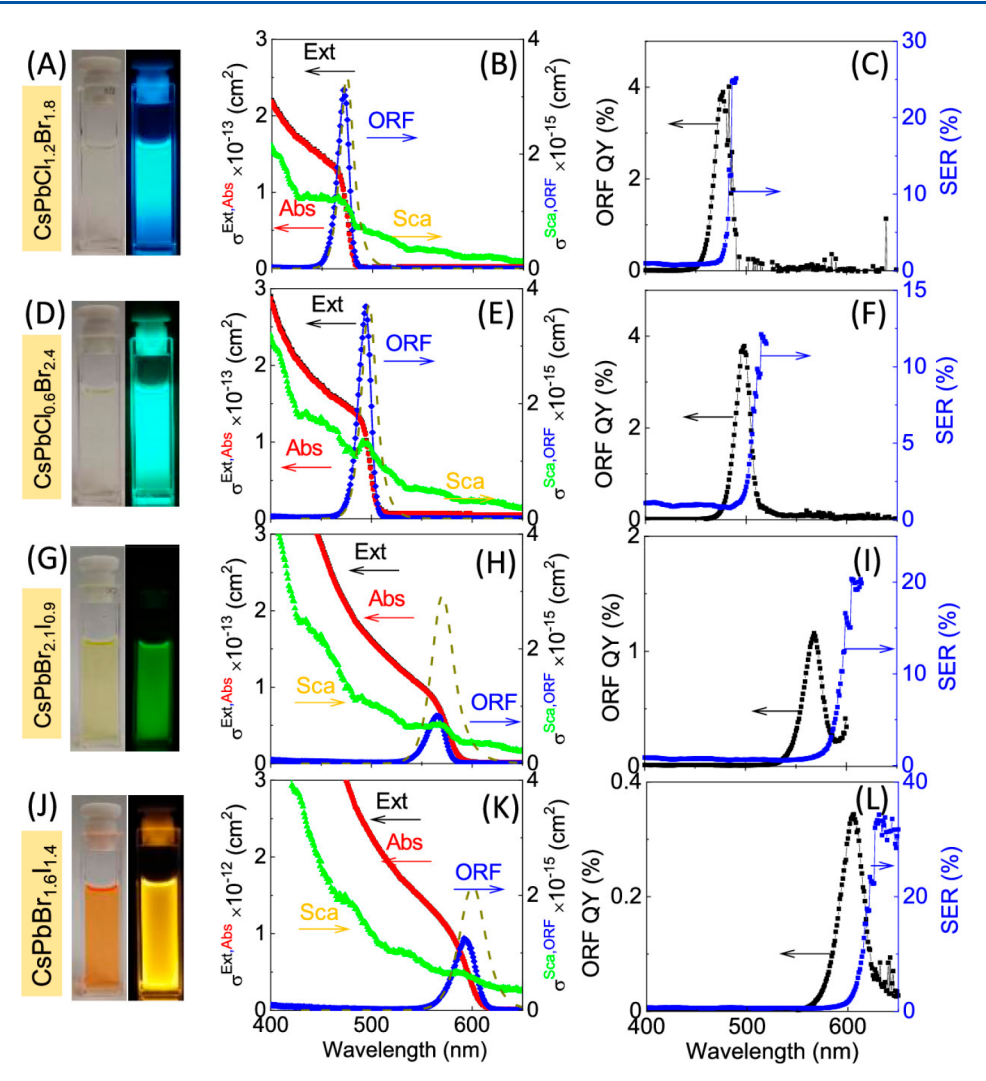


Figure 7. (first column) PNC composition in vertical-form, bright-field, and fluorescence photographs. (second column) UV-vis extinction (black), absorption (red), scattering (green), and ORF cross-section spectra. Dashed lines indicate the SSF emission spectra. (third column) ORF QY (black) and the SER spectra (blue). PNCs: (A-C) CsPbCl_{1.2}Br_{1.8}, (D-F) CsPbCl_{0.6}Br_{2.4}, (G-I) CsPbBr_{2.1}I_{0.9}, and (J-L) CsPbBr_{1.6}I_{1.6}⁵⁷

ORF. ^{56,57} In such cases, assigning the resonance synchronous spectrum as an RLS leads to the misclassification of the ORF as scattering or resonance scattering. Further, resonance light scattering refers to elastic scattering that occurs when the incident photons are close to the absorption band. ^{99,103,104} Even for the resonance synchronous features that are known to originate from scattering, assigning scattering as the resonance scattering requires further justifications.

ORF as a New Tool for Materials Characterization. With their expanding capabilities, it is now straightforward to use commercial spectrofluorometers to acquire the fluorophore ORF spectra and determining the ORF peak wavelength, bandwidth (full width at half-maximum), emission depolarization, and emission cross-section. Empirically, the ORF spectra obtained to date with molecular and nanoparticle fluorophores (Figure 7) all comprise of a single Gaussian peak. The successful acquisition of the ORF features paves the way for addressing questions on how the ORF encodes the materials' structural characteristics and optical properties. One significant question in nano research pertains to the determination of the bandgaps of photoelectronic nanomaterials, 65–67 which represent the minimum energy required for an electron to transition from the valence band to

the conduction band. The current method used to calculate these bandgaps relies on the red-edge UV—vis spectrum wavelength. However, these aspects face two main issues. First, the red-edge UV—vis wavelength does not necessarily correspond to the red-edge absorption wavelength, as nanoparticle UV—vis spectra often include both scattering and absorption contributions, and scattering is a universal property across the entire electromagnetic wavelength range. Second, the red-edge absorption wavelength is subjective and can vary depending on instrumental sensitivity, sampling conditions, and the user's chosen threshold for determining significant UV—vis transitions.

However, ORF can serve as a robust and objective method for measuring the bandgap of fluorescent nanoparticles. This approach enables cross-validation among different researchers, ensuring consistent and reliable determination of the bandgap. A Gaussian fitting of ORF features will produce peak ORF wavelength and bandwidth (full width at half-maximum (fwhm)). One possible way is to use the fitted ORF peak wavelength to calculate the materials' bandgaps. Another approach is to report the range of bandgap defined by the ORF peak wavelength and fwhm. The latter method offers an advantage, as it states the fact that the onset of the electronic

transition depends on the Boltzmann distribution of materials at their ground electronic states. Evidently, substantial future work is needed for the nano- and measurement science community to develop a consensus on the ORF-based bandgap quantification.

Another question that remains to be answered is the ORF sensitivity to the sizes, shapes, and compositions of fluorescence nanoparticles such as semiconductor quantum dots, perovskite nanoparticles, and metal clusters. We hypothesize that ORF from monodispersed nanocrystals comprise signal Gaussian peaks, while the polydispersed nanocrystals will have broad spectral peaks that require peak fitting with multiple Gaussian peaks. Testing this hypothesis, however, requires improvement in the instrument capability for improving the ORF spectral acquisition and high precision nanofabrication.

Scattering Depolarization Spectroscopy as an Emerging Analytical Technique. The sensitivity of light scattering depolarization to the sizes, shapes, refractive index, and concentrations of the scattering particles, as well as the wavelength of incident light, has long been established. Historically, however, the quantification of scattering depolarization has been difficult, as it was implemented majorly by home-developed instrumentation and has often been used for quantification of scattering depolarization at one specific laser wavelength, which limits the accessibility and information content of the technique. The advent of LPRS and LPAOS spectroscopic techniques enables routine acquisition of sample scattering depolarization spectra with commonly accessible instruments, which opens doors for exploring the utility of scattering depolarization spectroscopy for materials characterization. To explore the full potential of scattering depolarization spectroscopy, however, a series of instrument and data analysis issues should be addressed. First, the limit-of-detection of the scattering depolarization performed using the commercial spectrofluorometer is ~0.01, which is inadequate for quantification of the scattering depolarization for spherical nanoparticles or small solvent molecules such as CCl4 (Figure S6), where the calculated scattering depolarization can be as small as $10^{-4.59,61,93}$ Second, the precision of the scattering depolarization measurement also needs to be improved to investigate its sensitivity to nanoparticle morphological features.

CONCLUSION

The century-old UV-vis spectrophotometry and spectrofluorometry have remained the most affordable and accessible tools in education, research, and technology development. Based on the recent advances in the understanding of photon/matter interactions, this Perspective provided an augmented Jablonski energy diagram that better captures the complexity of the optical processes that can occur in spectroscopic measurements in nano research compared to the conventional Jablonski diagram. The roadmaps offered and the technology summarized in this work should enhance the evidence-based data interpretation of UV-vis and fluorescence spectroscopic techniques in student education and research. The casual and mostly erroneous usage of the terminology has been detrimental for promoting critical thinking for student education and scientific rigor in research. We strongly urge the research community to use methodology-based nomenclature, instead of the ones with connation to the photophysical

origins of the measurement signal to refer to the experimental spectrum. The spectral assignment should be performed only after verification of the reliability of the measurement data and be supported by experimental evidence. The latter has now become possible with the new measurement technologies recently developed with broadly accessible UV—vis and fluorescence instruments. Through a targeted focus on the critical issues related to UV—vis and fluorescence properties of nanomaterials, we hope this Perspective can serve as a valuable resource for researchers, educators, and practitioners. By promoting evidence-based approaches and improving the understanding of the limitations and opportunities with spectroscopic techniques, we seek to push the boundaries of optical spectroscopy and pave the way for groundbreaking discoveries in the exciting domain of nanoscience.

ASSOCIATED CONTENT

Supporting Information

The Supporting Information is available free of charge at https://pubs.acs.org/doi/10.1021/acs.analchem.3c03490.

Experimental linear dynamic range of UV—vis and integrating sphere UV—vis; example of inner-filter effect correction using a first-principles model; fluorescence and UV—vis spectral deviation for eosin Y mixed with polystyrene nanoparticles; experimental setup for linearly polarized spectra; AuNS quantified using LPRS methodology; and scattering cross section of solvents using LPRS (PDF)

AUTHOR INFORMATION

Corresponding Author

Dongmao Zhang — Department of Chemistry, Mississippi State University, Starkville, Mississippi 39762, United States; oorcid.org/0000-0002-2303-7338; Email: dongmao@chemistry.msstate.edu

Authors

Max Wamsley — Department of Chemistry, Mississippi State University, Starkville, Mississippi 39762, United States;

⊚ orcid.org/0000-0001-6790-4846

Shengli Zou — Department of Chemistry, University of Central Florida, Orlando, Florida 32816, United States;
orcid.org/0000-0003-1302-133X

Complete contact information is available at: https://pubs.acs.org/10.1021/acs.analchem.3c03490

Notes

The authors declare no competing financial interest.

ACKNOWLEDGMENTS

This work was supported in part by the Center of Biomedical Research Excellence Program funded through the Center for Research Capacity Building in the National Institute for General Medical Sciences (P20GM103646) and by an NSF Grant (CHE 2203571). S.Z. is grateful for the support from NSF (DMR-2004546). The content is solely the responsibility of the authors and does not necessarily represent the official views of the National Institutes of Health or National Science Foundation.

REFERENCES

- (1) Chinen, A. B.; Guan, C. M.; Ferrer, J. R.; Barnaby, S. N.; Merkel, T. J.; Mirkin, C. A. Chem. Rev. 2015, 115 (19), 10530–10574.
- (2) Wang, Z.; Wang, W.; Wamsley, M.; Zhang, D.; Wang, H. ACS Appl. Mater. Interfaces. 2022, 14 (15), 17560-17569.
- (3) Nasrollahpour, H.; Sánchez, B. J.; Sillanpää, M.; Moradi, R. ACS Appl. Nano Mater. 2023, 6 (14), 12609–12672.
- (4) Mosquera, J.; Wang, D.; Bals, S.; Liz-Marzán, L. M. Acc. Chem. Res. 2023, 56 (10), 1204–1212.
- (5) Metcalf, I.; Sidhik, S.; Zhang, H.; Agrawal, A.; Persaud, J.; Hou, J.; Even, J.; Mohite, A. D. *Chem. Rev.* **2023**, 123, 9565.
- (6) Shen, J.; Xu, B.; Chen, S.; Jia, Y.; Li, J.; Jiang, T.; Gao, Z.; Wang, X.; Zhu, C.; Shi, H.; Wang, Z. ACS Sustainable Chem. Eng. 2022, 10 (47), 15599–15607.
- (7) Vairaperumal, T.; Huang, C.-C.; Liu, P.-Y. ACS Appl. Bio Mater. **2023**, 6 (7), 2591–2613.
- (8) Mie, G. Ann. Phys. 1908, 330, 377-445.
- (9) Bohren, C. F.; Huffman, D. R. Absorption and Scattering of Light by Small Particles; John Wiley & Sons Inc.: New York, 1983.
- (10) Nawalage, S.; Wathudura, P.; Wang, A.; Wamsley, M.; Zou, S.; Zhang, D. Anal. Chem. 2023, 95 (3), 1899–1907.
- (11) Wathudura, P.; Wamsley, M.; Wang, A.; Chen, K.; Nawalage, S.; Wang, H.; Zou, S.; Zhang, D. *Anal. Chem.* **2023**, 95 (9), 4461–4469.
- (12) Wamsley, M.; Wathudura, P.; Nawalage, S.; Zou, S.; Zhang, D. Anal. Chem. 2023, 95 (27), 10279–10288.
- (13) Shen, Y.-F.; Zhang, H.; Zhang, J.; Tian, C.; Shi, Y.; Qiu, D.; Zhang, Z.; Lu, K.; Wei, Z. Adv. Mater. 2023, 35 (10), 2209030.
- (14) Song, M.; Xing, J.; Cai, H.; Gao, X.; Li, C.; Liu, C.; Li, X.; Fu, X.; Ding, S.; Cheng, W.; Chen, R. ACS Nano 2023, 17 (11), 10748–10759.
- (15) Du, K.; Wang, Y. J. Am. Chem. Soc. 2023, 145 (19), 10763-10778.
- (16) Kleine-Kleffmann, L.; Stepanenko, V.; Shoyama, K.; Wehner, M.; Würthner, F. J. Am. Chem. Soc. 2023, 145 (16), 9144–9151.
- (17) Wang, J.; Wang, L.; Su, X.; Yu, H. ACS Appl. Nano Mater. 2023, 6 (13), 12231–12239.
- (18) Yan, L.-L.; Wing-Wah Yam, V. J. Am. Chem. Soc. 2023, 145 (13), 7454–7461.
- (19) Yu, H.; Wang, D.; Jin, H.; Wu, P.; Wu, X.; Chu, D.; Lu, Y.; Yang, X.; Xu, H. Adv. Funct. Mater. 2023, 33 (24), 2214828.
- (20) Xu, J. X.; Hu, J.; Zhang, D. Anal. Chem. 2018, 90 (12), 7406-7414.
- (21) Xu, J. X.; Yuan, Y.; Zou, S.; Chen, O.; Zhang, D. Anal. Chem. 2019, 91 (13), 8540-8548.
- (22) Xu, J. X.; Niu, G.; Tang, B. Z.; Zhang, D. Journal of Materials Chemistry C 2019, 7 (39), 12086–12094.
- (23) Pugliese, M.; Scarfiello, R.; Prontera, C. T.; Giannuzzi, R.; Bianco, G. V.; Bruno, G.; Carallo, S.; Mariano, F.; Maggiore, A.; Carbone, L.; Gigli, G.; Maiorano, V. ACS Sustainable Chem. Eng. 2023, 11 (26), 9601–9612.
- (24) Ma, Q.; Zhang, Y.; Huangfu, Y.; Gao, S.; Zhou, C.; Rong, H.; Deng, L.; Dong, A.; Zhang, J. ACS Appl. Mater. Interfaces. 2023, 15 (9), 12209–12220.
- (25) Knežević, N. Ž.; Ilić, N.; Dokić, V.; Petrović, R.; Janaćković, D. o. e. ACS Appl. Mater. Interfaces. 2018, 10 (24), 20231–20236.
- (26) Chiu, N.-C.; Nord, M. T.; Tang, L.; Lancaster, L. S.; Hirschi, J. S.; Wolff, S. K.; Hutchinson, E. M.; Goulas, K. A.; Stickle, W. F.; Zuehlsdorff, T. J.; Fang, C.; Stylianou, K. C. *Chem. Mater.* **2022**, 34 (19), 8798–8807.
- (27) Vuong, H.-T.; Nguyen, D.-V.; Ly, P. P.; Phan, P. D. M.; Nguyen, T. D.; Tran, D. D.; Mai, P. T.; Hieu, N. H. ACS Appl. Nano Mater. **2023**, 6 (1), 664–676.
- (28) Yang, X.; Wang, D. ACS Appl. Energy Mater. 2018, 1 (12), 6657–6693.
- (29) Li, J.; Liu, Q.; Wang, P.; Zhang, L.; Fang, Y. ACS Appl. Nano Mater. 2023, 6 (5), 3211–3217.
- (30) Wang, J.; Zhou, B.; Ma, J.; Hu, X.; Xu, Y.; Huang, P.; Song, E.; Wang, L.; Jiang, W. ACS Appl. Nano Mater. 2023, 6 (1), 61-75.

- (31) Li, M.; Chen, T.; Gooding, J. J.; Liu, J. ACS Sens. 2019, 4 (7), 1732–1748.
- (32) Yan, L.; Liao, C.; Zhu, Y.; Mi, H.; Jiang, S.; Shan, F.; Liu, Y.; Zhang, Y.; Zhou, Q.; Wang, Z.; Yu, X. ACS Appl. Nano Mater. 2023, 6 (14), 13320–13329.
- (33) Wang, J.; Gu, Y.; Fan, Y.; Yang, M. ACS Appl. Nano Mater. 2023, 6 (14), 13561-13569.
- (34) Singh, S. K.; Mazumder, S.; Vincy, A.; Hiremath, N.; Kumar, R.; Banerjee, I.; Vankayala, R. ACS Appl. Nano Mater. 2023, 6 (3), 1508–1521.
- (35) Panigrahy, S.; Panda, P.; Shekhawat, A.; Barman, S. ACS Appl. Nano Mater. **2023**, 6 (5), 3825–3834.
- (36) Jokar, E.; Cai, L.; Han, J.; Nacpil, E. J. C.; Jeon, I. Chem. Mater. **2023**, 35 (9), 3404–3426.
- (37) Park, C.; Han, S. H.; Jin, H. J.; Hong, W.; Choi, S.-Y. ACS Nano **2023**, 17 (10), 9262–9271.
- (38) Lan, K.; Liu, L.; Yu, J.; Ma, Y.; Zhang, J.-Y.; Lv, Z.; Yin, S.; Wei, Q.; Zhao, D. *JACS Au.* **2023**, 3 (4), 1141–1150.
- (39) Lv, C.; Bai, X.; Ning, S.; Song, C.; Guan, Q.; Liu, B.; Li, Y.; Ye, J. ACS Nano 2023, 17 (3), 1725–1738.
- (40) Liu, J.; Wang, L.; Jia, T.; Wang, Z.; Xu, T.; An, N.; Zhao, M.; Zhang, R.; Zhao, X.; Li, C. ACS. Appl. Mater. Interfaces. 2023, 15, 37609.
- (41) Cui, X.; Ruan, Q.; Zhuo, X.; Xia, X.; Hu, J.; Fu, R.; Li, Y.; Wang, J.; Xu, H. Chem. Rev. 2023, 123 (11), 6891–6952.
- (42) Krasnok, A. E.; Miroshnichenko, A. E.; Belov, P. A.; Kivshar, Y. S. Opt. Express. 2012, 20 (18), 20599–20604.
- (43) Oelkrug, D.; Brun, M.; Rebner, K.; Boldrini, B.; Kessler, R. Appl. Spectrosc. **2012**, 66 (8), 934–943.
- (44) Fu, Y. H.; Kuznetsov, A. I.; Miroshnichenko, A. E.; Yu, Y. F.; Luk'yanchuk, B. Nat. Commun. 2013, 4 (1), 1527.
- (45) Wamsley, M.; Wathudura, P.; Hu, J.; Zhang, D. Anal. Chem. 2022, 94 (33), 11610–11618.
- (46) Valeur, B.; Berberan-Santos, M. N. Molecular Fluorescence: Principles and Applications; Wiley, 2012.
- (47) Lakowicz, J. R., Fluorescence Anisotropy. In *Principles of Fluroescence Spectroscopy*, 2 ed.; Lakowicz, J. R., Ed.; Springer Science: New York, 1999; pp 291–320.
- (48) Liu, B.-J.; Lin, K.-Q.; Hu, S.; Wang, X.; Lei, Z.-C.; Lin, H.-X.; Ren, B. Anal. Chem. 2015, 87 (2), 1058–1065.
- (49) Nelson, N. B.; Prézelin, B. B. Appl. Opt. 1993, 32 (33), 6710-6717.
- (50) Sun, L.; Bolton, J. R. J. Phys. Chem. 1996, 100 (10), 4127–4134.
- (51) Gaigalas, A. K.; He, H.-J.; Wang, L. J. Res. Natl. Inst. Stand. Technol. 2009, 114 (2), 69–81.
- (52) Mann, S. A.; Sciacca, B.; Zhang, Y.; Wang, J.; Kontoleta, E.; Liu, H.; Garnett, E. C. ACS Nano 2017, 11 (2), 1412–1418.
- (53) Mori, A.; Yamashita, K.; Tabata, Y.; Seto, K.; Tokunaga, E. Rev. Sci. Instrum. **2021**, 92 (12), 123103.
- (54) Lee, J.; Ryu, H.; Park, S.; Cho, M.; Choi, T.-L. *J. Am. Chem. Soc.* **2023**, *145* (28), *15488*–*15495*.
- (55) Wang, J.; Peled, T. S.; Klajn, R. J. Am. Chem. Soc. 2023, 145 (7), 4098-4108.
- (56) Siriwardana, K.; Vithanage, B. C. N.; Zou, S.; Zhang, D. Anal. Chem. 2017, 89 (12), 6686–6694.
- (57) Zhang, W.; Zilevu, D.; Creutz, S. E.; Zhang, D. J. Phys. Chem. C **2020**, 124 (37), 20388–20397.
- (58) Zhao, Y.; Hu, Y.; Zhong, Y.; Wang, J.; Liu, Z.; Bai, F.; Zhang, D. J. Phys. Chem. C **2021**, 125 (40), 22318–22327.
- (59) Xu, J. X.; Yuan, Y.; Liu, M.; Zou, S.; Chen, O.; Zhang, D. Anal. Chem. **2020**, 92 (7), 5346–5353.
- (60) Siriwardana, K.; Nettles, C. B., II; Vithanage, B. C. N.; Zhou, Y.; Zou, S.; Zhang, D. *Anal. Chem.* **2016**, *88* (18), 9199–9206.
- (61) Xu, J. X.; Siriwardana, K.; Zhou, Y.; Zou, S.; Zhang, D. Anal. Chem. **2018**, 90 (1), 785–793.
- (62) Bootharaju, M. S.; Lee, C. W.; Deng, G.; Kim, H.; Lee, K.; Lee, S.; Chang, H.; Lee, S.; Sung, Y.-E.; Yoo, J. S.; Zheng, N.; Hyeon, T. *Adv. Mater.* **2023**, *35* (18), 2207765.

- (63) Geng, H.; Lupton, E. J.; Ma, Y.; Sun, R.; Grigsby, C. L.; Brachi, G.; Li, X.; Zhou, K.; Stuckey, D. J.; Stevens, M. M. Adv. Healthc. Mater. 2023, 12 (27), 2301148.
- (64) Li, X.; Li, Y.; Yu, C.; Bao, H.; Cheng, S.; Huang, J.; Zhang, Z. ACS Nano 2023, 17 (7), 6387–6399.
- (65) Cicirello, G.; Wang, M.; Sam, Q. P.; Hart, J. L.; Williams, N. L.; Yin, H.; Cha, J. J.; Wang, J. J. Am. Chem. Soc. **2023**, 145 (14), 8218–8230.
- (66) Zhang, Y.; Yang, X.; Dai, Y.; Yu, W.; Yang, L.; Zhang, J.; Yu, Q.; Dong, Z.; Huang, L.; Chen, C.; Hou, X.; Wang, X.; Li, J.; Zhang, K. ACS Nano 2023, 17 (9), 8743–8754.
- (67) Cao, F.; Deng, X.; Liu, X.; Su, L.; Hong, E.; Wu, L.; Fang, X. ACS Appl. Mater. Interfaces. 2023, 15 (23), 28158–28165.
- (68) Ye, X.; Chung, L.-H.; Li, K.; Zheng, S.; Wong, Y.-L.; Feng, Z.; He, Y.; Chu, D.; Xu, Z.; Yu, L.; He, J. Nat. Commun. 2022, 13 (1), 6116
- (69) Jiang, H.; Yu, X.; Guo, M.; Yao, Y.-R.; Meng, Q.; Echegoyen, L.; Autschbach, J.; Chen, N. J. Am. Chem. Soc. **2023**, 145 (10), 5645–5654
- (70) Liu, Y.; Wang, J.; Li, L.; Meng, S.; Ji, K.; Ma, P.; Wang, J.; Niu, J. Chem. Mater. **2023**, 35 (10), 3941–3950.
- (71) Skoog, D. A.; Holler, F. J.; Crouch, S. R. Principles of Instrumental Analysis; Cengage Learning: New York, 2017; Vol. 7.
- (72) Wamsley, M.; Nawalage, S.; Hu, J.; Collier, W. E.; Zhang, D. Anal. Chem. 2022, 94 (19), 7123-7131.
- (73) Wamsley, M.; Peng, W.; Tan, W.; Wathudura, P.; Cui, X.; Zou, S.; Zhang, D. ACS Meas. Sci. Au. 2023, 3 (1), 10–20.
- (74) Xu, J. X.; Vithanage, B. C. N.; Athukorale, S. A.; Zhang, D. Analyst. 2018, 143 (14), 3382–3389.
- (75) Lakowicz, J. R. Fluorescence Quenching. In *Principles of Fluroescence Spectroscopy*, 2 ed.; Lakowicz, J. R., Ed.; Springer Science: New York, 1999; p 11.
- (76) Gehlen, M. H. J. Photochem. Photobiol. C 2020, 42, 100338.
- (77) Zhang, D.; Nettles, C. B. J. Phys. Chem. C 2015, 119 (14), 7941-7948.
- (78) Lakowicz, J. R. Instrumentation for Fluorescence Spectroscopy. In *Principles of Fluroescence Spectroscopy*, 2 ed.; Lakowicz, J. R., Ed.; Springer Science: New York, 1999; pp 25–61.
- (79) Tavakkoli Yaraki, M.; Liu, B.; Tan, Y. N. Nano-Micro Lett. 2022, 14 (1), 123.
- (80) Ribeiro, D. S.; Santos, J. C. C.; Grieger, S.; Campos, J. L. E.; Machado, L. R. P.; Pacheco, F. G.; Fernandes, T. F. D.; Haase, C. C.; Silva, D. L.; Guterres, M.; Soares, E. M.; Martins, R. M.; Del'Boccio, J. P.; Altoé, R.; Plentz, F.; Santos, A. P.; Furtado, C. A.; Vilela Neto, O. P.; Mazzoni, M. S. C.; Alves, E. S.; Neves, B. R. A.; Backes, C.; Cançado, L. G. ACS Appl. Nano Mater. 2023, 6 (13), 11198–11210.
- (81) Wolfbeis, O. S. Chem. Soc. Rev. 2015, 44 (14), 4743-4768.
- (82) Li, S.; Ma, R.; Xu, S.; Zheng, T.; Fu, G.; Wu, Y.; Liao, Z.; Kuang, Y.; Hou, Y.; Wang, D.; Petkov, P. S.; Simeonova, K.; Feng, X.; Wu, L.-Z.; Li, X.-B.; Zhang, T. J. Am. Chem. Soc. 2022, 144 (30), 13953—13960.
- (83) Hameed, F.; Mohanan, M.; Ibrahim, N.; Ochonma, C.; Rodríguez-López, J.; Gavvalapalli, N. *Macromolecules* **2023**, *56* (9), 3421–3429.
- (84) Zhang, J.; Li, J.; Ye, Z.; Cui, J.; Peng, X. J. Am. Chem. Soc. 2023, 145 (25), 13938–13949.
- (85) Richardson, B. J.; Zhang, C.; Rauthe, P.; Unterreiner, A.-N.; Golberg, D. V.; Poad, B. L. J.; Frisch, H. J. Am. Chem. Soc. 2023, 145 (29), 15981–15989.
- (86) Fernandes, R. S.; Dey, N. ACS Appl. Nano Mater. 2023, 6 (7), 5168-5176.
- (87) He, F.; Bai, J.; Cheng, Y.; Weerasinghe, K.; Meng, X.; Xu, H.; Zhang, W.; Fang, X.; Li, H.-B.; Ding, T. J. Phys. Chem. C 2021, 125 (9), 5207–5216.
- (88) Lakowicz, J. R. Principles of Fluroescence Spectroscopy, 2 ed.; Springer Science: New York, 1999.
- (89) Ren, X.-R.; Bai, B.; Zhang, Q.; Hao, Q.; Guo, Y.; Wan, L.-J.; Wang, D. J. Am. Chem. Soc. 2022, 144 (6), 2488–2494.

- (90) Katzbaer, R. R.; dos Santos Vieira, F. M.; Dabo, I.; Mao, Z.; Schaak, R. E. J. Am. Chem. Soc. 2023, 145 (12), 6753-6761.
- (91) Berkson, Z. J.; Zhu, R.; Ehinger, C.; Lätsch, L.; Schmid, S. P.; Nater, D.; Pollitt, S.; Safonova, O. V.; Björgvinsdóttir, S.; Barnes, A. B.; Román-Leshkov, Y.; Price, G. A.; Sunley, G. J.; Copéret, C. J. Am. Chem. Soc. 2023, 145 (23), 12651–12662.
- (92) Majher, J. D.; da Cruz Pinha Barbosa, V.; Chae, C.; Strom, T. A.; Hwang, J.; Woodward, P. M. Chem. Mater. 2023, 35 (2), 482–489.
- (93) Athukorale, S. A.; Zhou, Y.; Zou, S.; Zhang, D. Anal. Chem. **2017**, 89 (23), 12705–12712.
- (94) Vithanage, B. C. N.; Xu, J. X.; Zhang, D. J. Phys. Chem. B 2018, 122 (35), 8429-8438.
- (95) Nettles, C. B., II; Zhou, Y.; Zou, S.; Zhang, D. Anal. Chem. **2016**, 88 (5), 2891–2898.
- (96) Zhang, Y.; He, S.-R.; Yang, Y.; Zhang, T.-S.; Zhu, Z.-M.; Fei, W.; Li, M.-B. *J. Am. Chem. Soc.* **2023**, *145* (22), 12164–12172.
- (97) Uva, A.; Lin, A.; Tran, H. J. Am. Chem. Soc. 2023, 145 (6), 3606-3614.
- (98) Muniz, C. N.; Archer, C. A.; Applebaum, J. S.; Alagaratnam, A.; Schaab, J.; Djurovich, P. I.; Thompson, M. E. J. Am. Chem. Soc. 2023, 145 (25), 13846–13857.
- (99) Pasternack, R. F.; Collings, P. J. Science. 1995, 269 (5226), 935-939.
- (100) Maiti, N. C.; Mazumdar, S.; Periasamy, N. J. Phys. Chem. B 1998, 102 (9), 1528-1538.
- (101) Kano, K.; Fukuda, K.; Wakami, H.; Nishiyabu, R.; Pasternack, R. F. J. Am. Chem. Soc. **2000**, 122 (31), 7494–7502.
- (102) Lovell, J. F.; Jin, C. S.; Huynh, E.; Jin, H.; Kim, C.; Rubinstein, J. L.; Chan, W. C. W.; Cao, W.; Wang, L. V.; Zheng, G. *Nat. Mater.* **2011**, *10* (4), 324–332.
- (103) Collings, P. J.; Gibbs, E. J.; Starr, T. E.; Vafek, O.; Yee, C.; Pomerance, L. A.; Pasternack, R. F. *J. Phys. Chem. B* **1999**, *103* (40), 8474–8481.
- (104) Jiang, X. Y.; Chen, X. Q.; Dong, Z.; Xu, M. J. Autom Methods Manag Chem. 2007, 2007, 1.
- (105) Tauc, J.; Grigorovici, R.; Vancu, A. Phys. Status Solidi B 1966, 15 (2), 627-637.
- (106) Duncan, D. D.; Thomas, M. E. Appl. Opt. 2007, 46 (24), 6185-6191.
- (107) Zhang, Y.-G.; Zhang, J.; Wu, S.-T.; Gao, J.-L.; Hao, Z.-Q.; Li, C.-L. Opt. Commun. 2022, 518, 128183.
- (108) Grynko, Y.; Shkuratov, Y. J. Quant. Spectrosc. Radiat. 2007, 106, 56-62.
- (109) Khlebtsov, N. G.; Mel'nikov, A. G.; Bogatyrev, V. A.; Alekseeva, A. V.; Khlebtsov, B. N. *Opt. Spectrosc.* **2006**, *100* (3), 448–
- (110) Chan, Y. C.; Wong, K. Y. J. Chem. Phys. 2012, 136 (17), 174514.
- (111) Zhang, Y.-G.; Zhang, J.; Wu, S.-T.; Gao, J.-L.; Hao, Z.-Q.; Li, C.-L. Opt. Commun. 2022, 518, 128183.